Comparative Medicine
Copyright 2021
by the American Association for Laboratory Animal Science

Vol 71, No 4
August 2021
Pages 285–294

Original Research

Relationships between *Slc1a5* and Osteoclastogenesis

Hideki Tsumura,[1,*,†] Miyuki Shindo,[1,†] Morihiro Ito,[2] Arisa Igarashi,[3] Kazue Takeda,[4] Kenji Matsumoto,[4] Takashi Ohkura,[5] Kenji Miyado,[5] Fumihiro Sugiyama,[6] Akihiro Umezawa,[5] and Yasuhiko Ito[2]

***Slc1a5* (*ASCT2*) encodes a small neutral amino-acid exchanger and is the most well-studied glutamine transporter in cancer cells. To investigate the role of *Slc1a5* in osteoclastogenesis, we developed *Slc1a5*-deficient mice by using a conventional gene-targeting approach. The *Slc1a5*$^{-/-}$ mice showed no obvious abnormalities in growth. Glutamine uptake was assessed in *Slc1a5*$^{+/+}$ and *Slc1a5*$^{-/-}$ bone marrow cells stimulated with RANKL. The rate of glutamine uptake in *Slc1a5*$^{-/-}$ bone marrow cells was reduced to 70% of that of cells from *Slc1a5*$^{+/+}$ bone marrow. To confirm the involvement of *Slc1a5* in osteoclast formation, bone marrow cells derived from *Slc1a5*$^{+/+}$ or *Slc1a5*$^{-/-}$ mice were stimulated with RANKL and macrophage colony-stimulating factor and stained with tartrate-resistant acid phosphatase. The bone resorption activity and actin ring formation of stimulated cells were measured. The formation of multinucleated osteoclasts in bone marrow cells isolated from *Slc1a5*$^{-/-}$ mice was severely impaired compared with those from *Slc1a5*$^{+/+}$ mice. RANKL-induced expression of ERK, NFκB, p70S6K, and NFATc1 was suppressed in *Slc1a5*$^{-/-}$ osteoclasts. These results show that *Slc1a5* plays an important role in osteoclast formation.**

Abbreviations: ASCT2, alanine serine cysteine transporter 2; mCSF, macrophage colony-stimulating factor

DOI: 10.30802/AALAS-CM-21-000012

Osteoclasts are giant multinucleated cells of hematopoietic origin that are responsible for bone resorption. The differentiation of osteoclasts can be induced by treating bone marrow macrophages with RANKL.[2] After stimulation, bone marrow macrophages mature and then fuse to become multinucleated osteoclasts. The processes of osteoclastogenesis and bone resorption are known to be energy-demanding,[8] but little is known about the amino acid requirements of osteoclasts. In this study, we investigated the role of glutamine in osteoclastogenesis. Glutamine was selected for this work because it provides an excellent example of amino acid metabolism.

Although glutamine acts as an essential amino acid in some specific physiologic situations, it is classified as a nonessential amino acid.[5] The need for the biosynthesis and metabolism of amino acids is significantly increased in cells with high rates of proliferation, such as functionally active cells and cancer cells. The activity of amino acid synthetases such as glutamine synthetase is increased in these cells. In addition, glutamine transporters on the plasma membrane are important, because they mediate glutamine uptake to meet the intracellular glutamine demand. The transporter *Slc1a5*, also known as ASCT2, is particularly important for glutaminolysis and mTOR signaling.[14,16]

Received: 26 Jan 2021. Revision requested: 10 Mar 2021. Accepted: 02 May 2021.
[1]Division of Laboratory Animal Resources, National Research Institute for Child Health and Development, Tokyo, Japan; [2]Department of Microbiology, College of life and Health Science, Chubu University, Aichi, Japan; Departments of [3]Genome Medicine, [4]Allergy and Clinical Immunology, and [5]Reproductive Biology, National Research Institute for Child Health and Development, Tokyo, Japan; and [6]Laboratory Animal Resource Center, Transborder Medical Research Center, Faculty of Medicine, University of Tsukuba, Ibaraki, Japan
[*]Corresponding author. Email: tsumura-h@ncchd.go.jp
[†]These authors contributed equally to this work

Glutamine concentrations in tissue and blood are regulated by the activities of glutamine synthetase and glutaminase. Endogenous synthesis cannot meet the cell's demands for glutamine in conditions including cancer, infections, and intense physical exercise. Glutamine is released into the blood from the lungs, adipocytes, and skeletal muscles and is transported into the cytoplasm via glutamine acid transporter molecules on the cell membrane. Glutamine is required for the growth of cancer cells; upregulation of the expression of the proteins involved in glutamine transport has been observed in tumor cells.[4]

Slc1a5 (ASCT2) is a small neutral amino acid exchanger that is overexpressed in many cancers and is the most well-described glutamine transporter in cancer cells.[9] However, previous studies[1,10,22,23] have reported that silencing, deletion, and amino-acid analog substitution of *Slc1a5* in cancer cells generated different results for mTORC1 signaling, proliferation, and cell migration.[1,3,4,10,22,23] Additional work[3,4] has shown that *Slc1a5* is indispensable for tumor growth and mTORC1 signaling. *Slc1a5* is important in accumulating nonessential amino acids to quickly restore amino acid composition during imbalanced amino acid usage,[4] whereas *Slc38a1* (SNAT1) and *Slc38a2* (SNAT2) mediate the net import of glutamine.

In bone homeostasis, glutamine is a critical regulator of energy for protein and nucleic acid synthesis via the tricarboxylic acid cycle. Active glutamine metabolism stimulates the proliferation and differentiation of osteoblasts, chondrocytes, and osteoclasts. The enzyme glutaminase deaminates glutamine to form glutamate. Glutaminase deficiency in osteoblasts and chondrocytes leads to reduced osteoblast formation and decreased bone mass, resulting in potentially dangerous conditions, such as osteoporosis.[24] In osteoclasts, glutamine is an important source of fuel for protein and nucleic acid biosynthesis. Therefore, *Slc1a5*

deficiency in mice may influence bone homeostasis, including osteoclastogenesis. We therefore created *Slc1a5*-deficient mice to investigate the contribution of *Slc1a5* to the development and functional properties of osteoclasts.

Materials and Methods

Ethics statement. All mice were housed at the animal facility of the National Research Institute for Child Health and Development, and all animal procedures were approved by the institution's Animal Care and Use Committee.

Mice. ICR and C57BL/6J mice were obtained from CLEA Japan (Tokyo, Japan). Room conditions in the animal facility were temperature, 20 to 24 ˚C, relative humidity, 50% ±20%; and 12:12-h light:dark photocycle. Mice were housed with unrestricted access to a standard diet (CE-2, CLEA Japan, Tokyo, Japan) and filter-sterilized water. They were housed in polycarbonate cages containing sterilized wood shaving. Nest material (Happi-mats, Marshall BioResources, Ibaraki, Japan) was provided during breeding.

The targeting vector pNT1.1 was provided by Dr Okabe (University of Osaka, Osaka, Japan). To ablate the *Slc1a5* gene from the mouse germline, we constructed a plasmid, pNT1.1, carrying the gene sequence but with the first exon replaced by a floxed neomycin resistance cassette. A genomic fragment of *Slc1a5* was used to make the targeting constructs for both the 5′ and 3′ arms. For the 5′ arm, a 4.2-kb 5′-flanking sequence of the *Slc1a5* gene was cloned into the SalI site of the pNT1.1 plasmid. For the 3′ arm, a 5.3-kb 3′-flanking sequence of the *Slc1a5* gene was cloned into the MfeI site. The linearized construct was electroporated into C57BL/6 mouse embryonic stem cells, which were already established,[20] and candidate clones were selected by using 200 µg/mL G418 for 7 d. All resistant embryonic stem cell clones were screened and confirmed to carry the *Slc1a5* sequence. The 5′ probe flanking the *Slc1a5* locus detected a 14-kb HindIII restriction fragment in wild-type mice and a 5.2-kb HindIII restriction fragment at the targeted locus, whereas the 3′ probe flanking the *Slc1a5* locus detected a 14-kb HindIII restriction fragment in wild-type mice and a 6.8-kb HindIII restriction fragment at the targeted locus (Figure 1). Southern blot hybridization using HindIII was employed to confirm the expected recombination in the embryonic stem cell clones. Several embryonic stem cell clones were independently aggregated with ICR 8-cell morula, followed by embryo transfer into the uteri of pseudopregnant ICR mice. Chimeric progeny were identified by their mosaic coat color. Intercrosses between the chimeric progeny and C57BL/6J mice were used to generate *Slc1a5*–neo mutant heterozygotes. The *Slc1a5*–neo mice were bred with flox deleter strain (Meox–Cre) mice, to excise the neomycin selection cassette. The strain was maintained by breeding $Slc1a5^{+/-}$ mice with prototype C57BL/6J or $Slc1a5^{+/-}$ mice. To identify the genotype of the mice, genomic PCR was performed by using 3 primers (Figure 1): primer 287 (5′ ATT GTT ATT CAC CCT AGG TT 3′), primer 353 (5′ ACT GGA GCC CTA GAA GGA GT 3′), and primer 354 (5′ CTT AGG GCA GTC CTT GTA TC 3′). The mRNA of *Slc1a5* was examined in bone marrow cells by using RT-PCR analysis, primer 307 (5′ AGT CTC CAG GCT CAC AAG GA 3′), and primer 308 (5′ CTG TGA CCA GGA TGG TGA TG 3′).

Bone µCT. All mice at 6 wk of age were euthanized by decapitation under sevoflurane anesthesia. After euthanasia, femurs and tibias were removed. The architecture and bone volume of the proximal femurs of all mice in the study were evaluated by using µCT (Kureha Special Laboratory, Fukushima, Japan).

Glutamine uptake. Bone marrow mononuclear cells isolated from the femurs and tibia of the mice were incubated in 24-well plates at 10^6 cells per well in αMEM containing 10% fetal bovine serum and 100 ng/mL macrophage colony-stimulating factor (mCSF). After preincubation for 3 d, the growth medium was removed, and bone marrow mononuclear cells were cultured with mCSF (100 ng/mL) and RANKL (200 ng/mL) for 1 d. This condition sufficiently induces *in vitro* osteoclast differentiation.[19] Glutamine uptake was measured by using a modification of the protocol described in a previous report.[6] The samples with or without RANKL stimulation were washed 3 times with modified Hanks balanced salt solution (Sigma–Aldrich, St Louis, MO). The cells were preloaded by the addition of 0.5 mL modified Hanks balanced salt solution containing [^{3}H]glutamine. After 10 min, samples were washed 3 times, and the cells were lysed by adding 1% Triton X100. The remaining radioactivity was determined by liquid scintillation counting. To measure Na^+-independent glutamine transport, NaCl was replaced by $LiCl_2$, and sodium phosphate was replaced by potassium phosphate in all buffers. An aliquot of the mixture was used for protein determination (Bio-Rad Protein Assay Kit, Bio-Rad, Hercules, CA).

Induction of osteoclasts. Bone marrow mononuclear cells at a concentration of 2×10^5 cells per well were cultured in the presence of 100 ng/mL mCSF and 200 ng/mL RANKL for 5 d. The cells were fixed with 10% paraformaldehyde. For TRAP staining of osteoclasts, the fixed cells were incubated for 30 min at 37 °C in acetate buffer (45mM sodium acetate, pH5.0) containing α-naphthol AS-MX phosphate (0.5mg/mL) and 50 mM sodium tartrate. Fast violet was used to visualize the product. To observe actin rings, cells were fixed and then washed with 0.2% Triton X100 in PBS before being incubated with 0.2 U/mL of rhodamine phalloidin (Molecular Probes). Rhodamine–phalloidin-stained actin rings were visualized under fluorescence microscopy.

Bone resorption assay. To examine resorption pit formation, bone marrow cells at a concentration of 1×10^5 cells per well were cultured for 7 d on dentine slices in 96-well plates that had been seeded 24 h earlier with UAMS32 cells (5×10^3 cells per well) in the presence of $1,25(OH)_2D_3$ (10^{-8} M). After 3 d, the culture medium and added factors were replenished daily. To quantify the resorption lacunae, cells were removed from the dentine slices by using mechanical agitation, and the bone slices were stained with 1% toluidine blue for 20 min. Resorption pits were observed under microscopy (ShuttlePix, Nikon, Tokyo, Japan).

Western blotting. Western blotting was performed using standard methods.[21] Blots were probed by using the following primary antibodies: antiβ-actin (catalog no. A1978, Sigma–Aldrich, St Louis, MO), phospho-ERK (catalog no. 4370, Cell Signaling Technology, Danvers, MA), ERK (catalog no. 4695, Cell Signaling Technology), phospho-p38 (catalog no. 4511, Cell Signaling Technology), p38 (catalog no. 9121, Cell Signaling Technology), phosho-p70SK6 (catalog no. 9234, Cell Signaling Technology), p70SK6 (catalog no. 2708, Cell Signaling Technology), phospho-RelA (catalog no. 3033, CST), RelA (catalog no. 8242, Cell Signaling Technology), and NFATc1 (catalog no. sc7294, Santa Cruz Biotechnology, Santa Cruz, CA).

Gene Chip analysis. Cy3-labeled cRNA transcripts were synthesized from 100 ng total RNA by using Low Input Quick Amp Labeling Kit (Agilent, Santa Clara, CA) according to the manufacturer's protocol. The fragmented samples were hybridized on a microarray slide (SurePrint G3 Mouse GE Microarray 8 × 60K, version 2.0, Agilent). The microarray slides were then scanned on a SureScan Microarray Scanner (Agilent), and the images were processed with Feature Extraction 10.7.3.1 software (Agilent). Data were analyzed by using GeneSpring GX

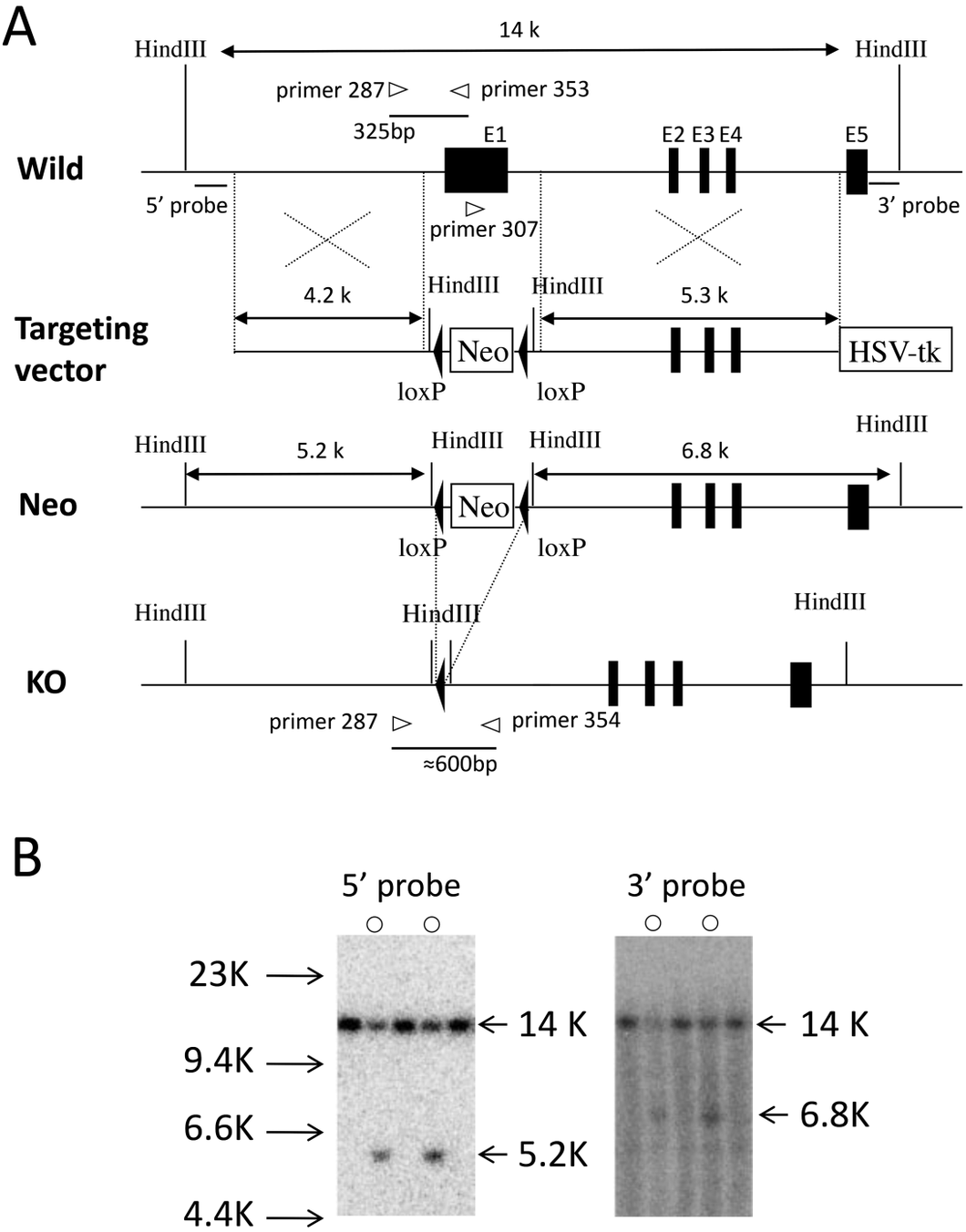

Figure 1. Targeted disruption of *Slc1a5*. (A) Targeting strategy via homologous recombination in embryonic stem cells. The structures of the wild-type *Slc1a5* (top), targeting vector (second), *neo* allele (third), and knockout allele (bottom) are shown. (B) Southern blot analysis of recombinant embryonic stem clones: genomic DNA was digested with HindIII and labeled with the 5′ and 3′ external probes.

(version.14.8, Agilent) which initially involved the removal of control probes and 75% shift normalization.

Statistical analysis. All data were expressed as individual values or as mean ± 1 SD. Welch tests were used for statistical analyses, and comparisons were made between *Slc1a5*$^{+/+}$ and *Slc1a5*$^{-/-}$ samples.

Results

Generation of *Slc1a5*-deficient mice. To prepare a model for studying the function of *Slc1a5*, we used a conventional gene-targeting method (Figure 1). To exclude the neo cassette, the *Slc1a5*$^{neo/+}$ mice were bred with a loxP deleter strain (Meox–Cre mice). The *Slc1a5*$^{+/-}$ mice were mated with each other; *Slc1a5*$^{-/-}$ mice were produced in the ratio expected according to Mendelian inheritance and did not show obvious abnormalities such as changes in growth, survival and reproductive function. Gene deletion was confirmed by using genomic PCR analysis, and *Slc1a5* mRNA was not detected in RT-PCR analysis of *Slc1a5*$^{-/-}$ bone marrow cells (Figure 2). Furthermore, the mRNA of *Slc1a5*$^{-/-}$ bone marrow cells was dramatically decreased

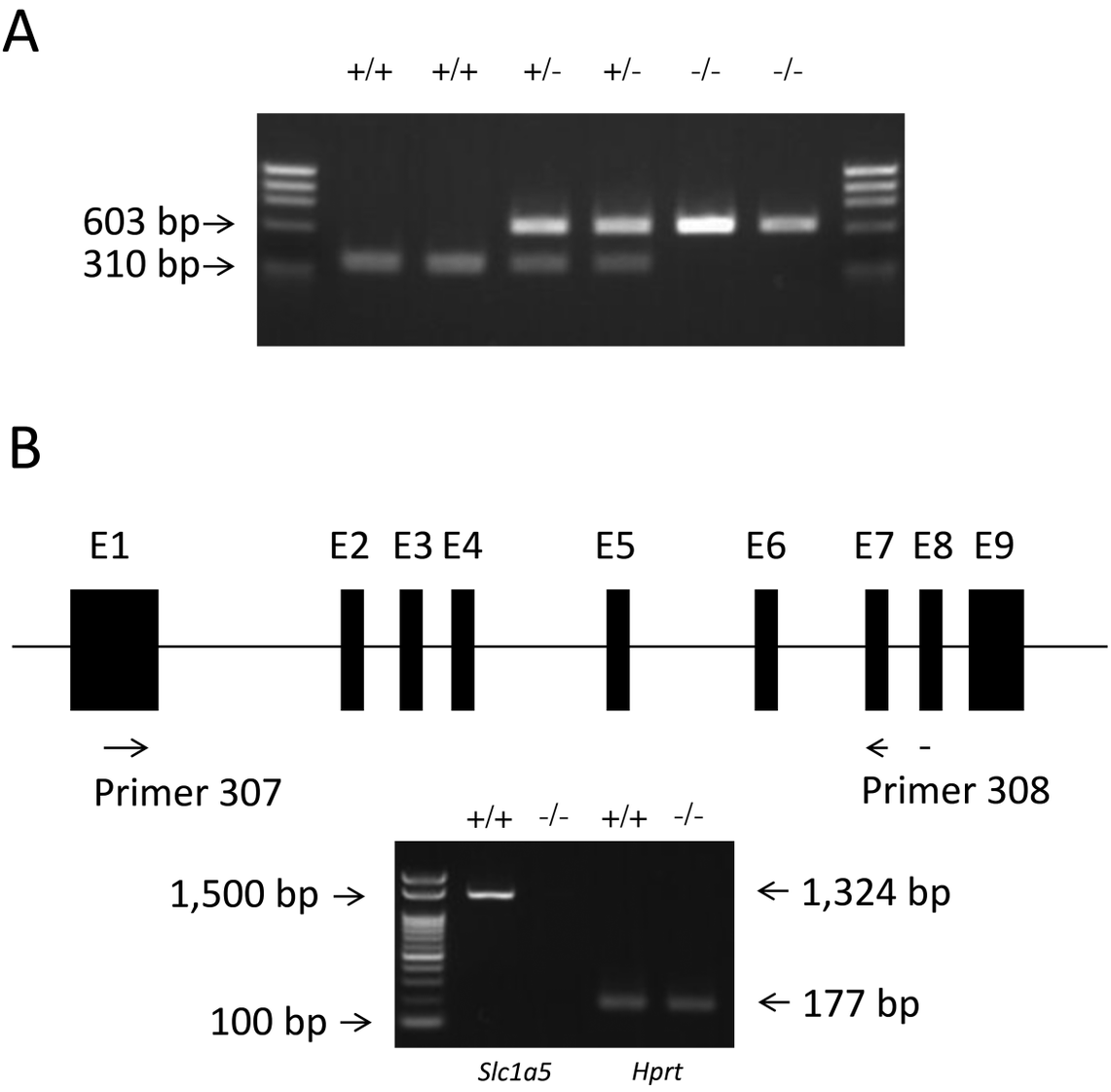

Figure 2. (A) PCR-based genotype analysis of mice. See Figure 1 A for primer sites. (B) RT-PCR analysis of RNA isolated from bone marrow cells. The expression of *Slc1a5* was undetectable in the bone marrow cells from *Slc1a5*$^{-/-}$ mice. The sequences for the *Hprt* primers are: primer 185, 5′ GTA ATG ATC AGT CAA CGG GGG AC 3′, and primer 186, 5′ CCA GCA AGC TTG CAA CCT TAA CCA 3′. The numbered black boxes indicate exons in *Slc1a5*.

based on Gene Chip analysis (*Slc1a5*$^{+/+}$, 2.81 ± 0.35 vs. *Slc1a5*$^{-/-}$, –7.62 ± 0.05; $P = 0.0001$; $n = 4$ per group).

Glutamine uptake in *Slc1a5*$^{-/-}$ bone marrow cells stimulated with RANKL. Glutamine transport through *Slc1a5* occurs in a Na^+-dependent manner. To assess *Slc1a5* function, glutamine uptake assays were performed on bone marrow cells stimulated with only mCSF for 3 d. The amount of glutamine taken up by the bone marrow cells isolated from *Slc1a5*$^{-/-}$ mice did not differ from that taken up by bone marrow cells isolated from *Slc1a5*$^{+/+}$ mice (Figure 3 A). The bone marrow cells were then stimulated with mCSF for 3 d, followed by incubation with mCSF and RANKL for 1 d. The rate of glutamine uptake in *Slc1a5*$^{-/-}$ bone marrow cells stimulated with RANKL was reduced to about 70% of that of *Slc1a5*$^{+/+}$ bone marrow cells in the presence of Na^+ (Figure 3 B). These findings imply that disruption of *Slc1a5* gene decreased glutamine uptake in *Slc1a5*$^{-/-}$ bone marrow cells.

Analysis of bone remodeling in *Slc1a5*$^{-/-}$ mice. To investigate the bone remodeling in *Slc1a5*$^{-/-}$ mice, we performed µCT analysis. No significant differences in bone/total ratio, trabecular thickness, trabecular number, and trabecular separation between *Slc1a5*$^{+/+}$ mice and *Slc1a5*$^{-/-}$ mice were observed. (Table 1).

Roles of *Slc1a5* in osteoclast formation. To study the roles of *Slc1a5* in osteoclast formation, we investigated the

Table 1. *Slc1a5* deletion suppressed RANKL-induced osteoclast differentiation. Bone histomorphometry of proximal tibia at 6 wk of age ($n = 5$ per genotype).

	+/+	-/-	*P*
BV/TV (%)	11.24 ± 2.05	13.52 ± 1.55	0.082
Tb.Th (µm)	31.94 ± 2.04	34.50 ± 2.47	0.111
Tb.N (mm^{-1})	3.48 ± 0.42	3.90 ± 0.25	0.096
TbSp (µm)	257.0 ± 35.3	221.6 ± 17.6	0.079

BV/TV: bone volume/total volume; Tb.Th, trabecular thickness; Tb.N, trabecular number; Tb.Sp, trabecular space.

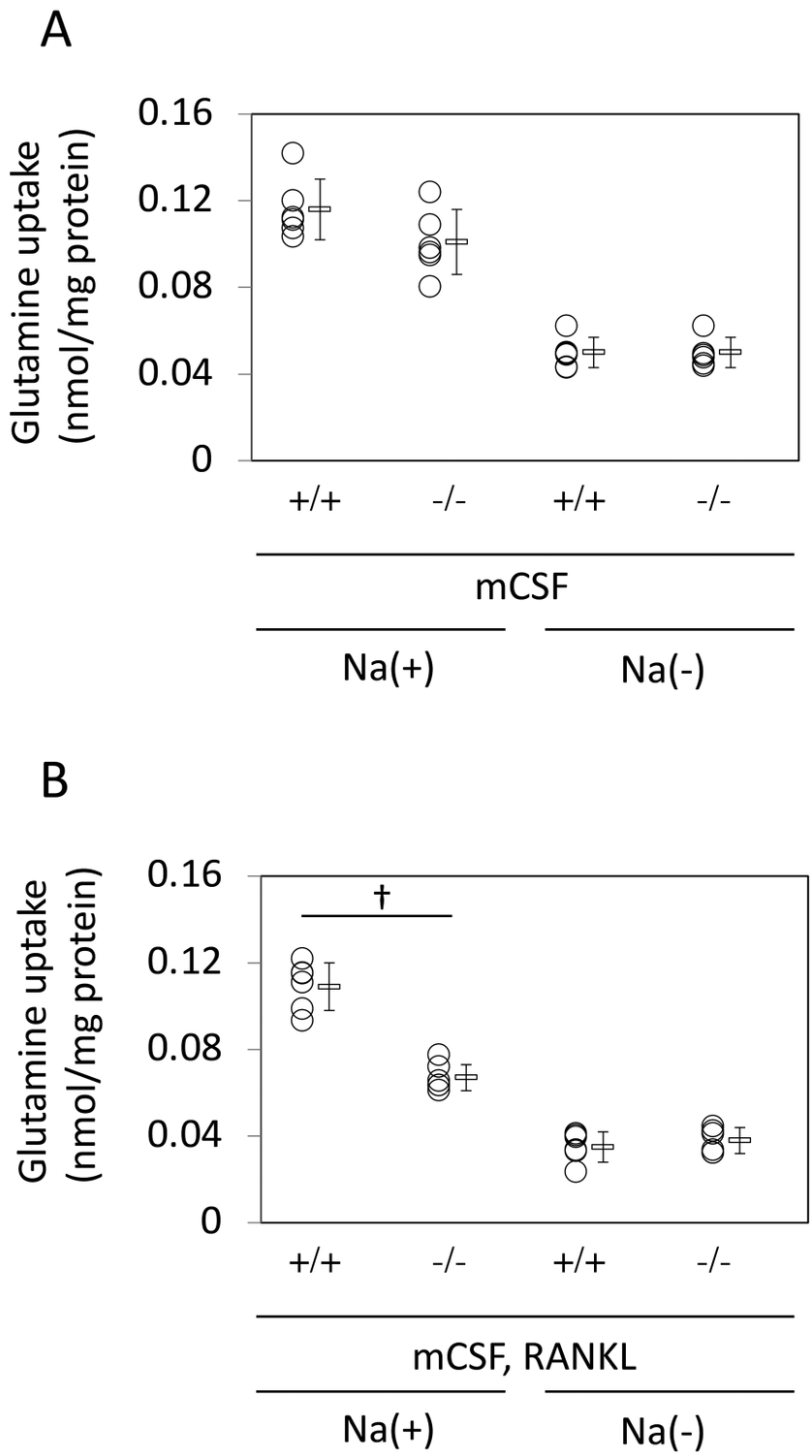

Figure 3. Glutamine uptake analysis in Na^+-containing or Na^+-free incubation buffer. (A) Glutamine uptake assays were performed in bone marrow cells stimulated with mCSF for 3 d. (B) Glutamine uptake in bone marrow cells incubated with mCSF for 3 d and then with mCSF and RANKL for 1 d. Glutamine uptake in the incubated cells derived from *Slc1a5*$^{+/+}$ and *Slc1a5*$^{-/-}$ mice is normalized to protein content (in milligrams). †, $P < 0.01$ between *Slc1a5*$^{+/+}$ mice and *Slc1a5*$^{-/-}$ mice ($n = 6$ per group).

osteoclastogenesis of bone marrow cells stimulated with mCSF and RANKL for 5 d. TRAP-positive osteoclasts were generated as expected from bone marrow cells derived from *Slc1a5*$^{+/+}$ mice, whereas TRAP-positive osteoclast formation was significantly lower ($P = 0.038$) in bone marrow cells derived from *Slc1a5*$^{-/-}$ mice (Figure 4 A). Actin ring formation and bone resorption were markedly different between the osteoclasts derived from *Slc1a5*$^{+/+}$ mice as compared with *Slc1a5*$^{-/-}$ mice

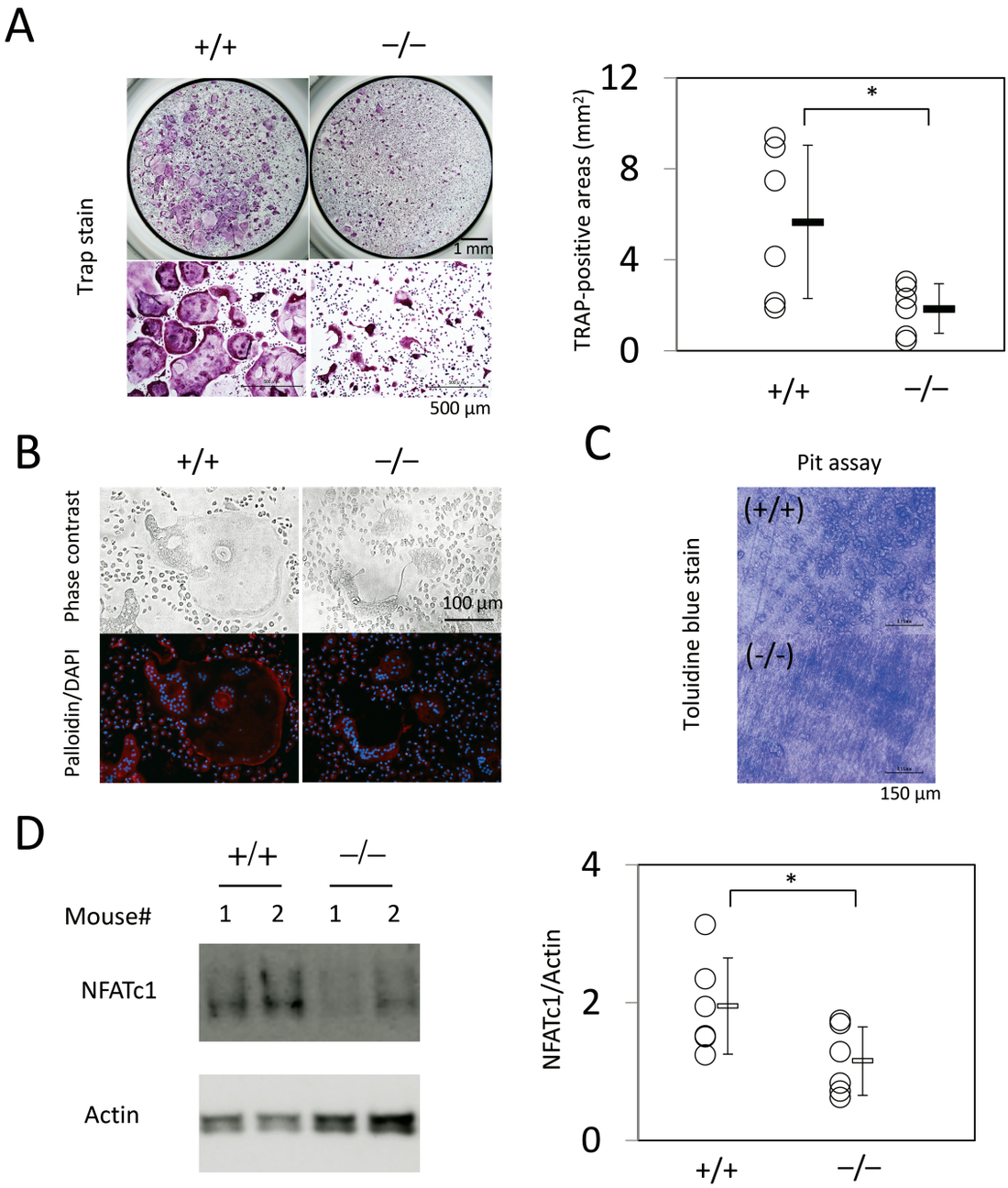

Figure 4. (A) Bone marrow cells were stimulated by mCSF and RANKL for 5 d. Cells were fixed and TRAP-stained. TRAP-positive areas were calculated by using the color extraction system of Hybrid Cell Count (Keyence, Osaka, Japan). (B) Actin ring formation. The fixed cells were stained with rhodamine phalloidin and DAPI. (C) Resorption pit formation. The bone slices were stained with 1% toluidine blue. (D) NFATc1 proteins were immunoblotted; actin served as a loading control. *, $P < 0.05$ between *Slc1a5*$^{+/+}$ mice and *Slc1a5*$^{-/-}$ mice ($n = 6$ per group).

(Figure 4 B and C), and the expression of NFATc1 was significantly lower ($P = 0.048$) in cells from the bone marrow of *Slc1a5*$^{-/-}$ mice (Figure 4 D).

Gene expression levels in osteoclasts derived from *Slc1a5*$^{-/-}$ mice. To further investigate the role of *Slc1a5* in osteoclastogenesis, we used the Gene Chip system to analyze the expression of multiple genes in RANKL-induced osteoclasts derived from *Slc1a5*$^{+/+}$ mice and *Slc1a5*$^{-/-}$ mice. The values represent the ratio of change related to osteogenesis and glutamine metabolism genes in bone marrow–derived macrophages as compared with osteoclasts. The expression of some genes, such as *Oscar* and *Calcr*, which are known to be high in osteoclasts, was significantly lower in osteoclasts derived from *Slc1a5*$^{-/-}$ mice as compared with *Slc1a5*$^{+/+}$ mice (Figure 5 A). However, we found no significant differences in the expression of genes related to the glutamine transporter (Figure 5 B), glutamine metabolism (Figure 5 C), amino acid starvation (Figure 5 D), or fusion factors (Figure 5 E) between the osteoclasts derived from the 2 genotypes of mice. Expression of the gene for matrix metalloproteinase 9 (*Mmp9*), one of the targets of ERK,

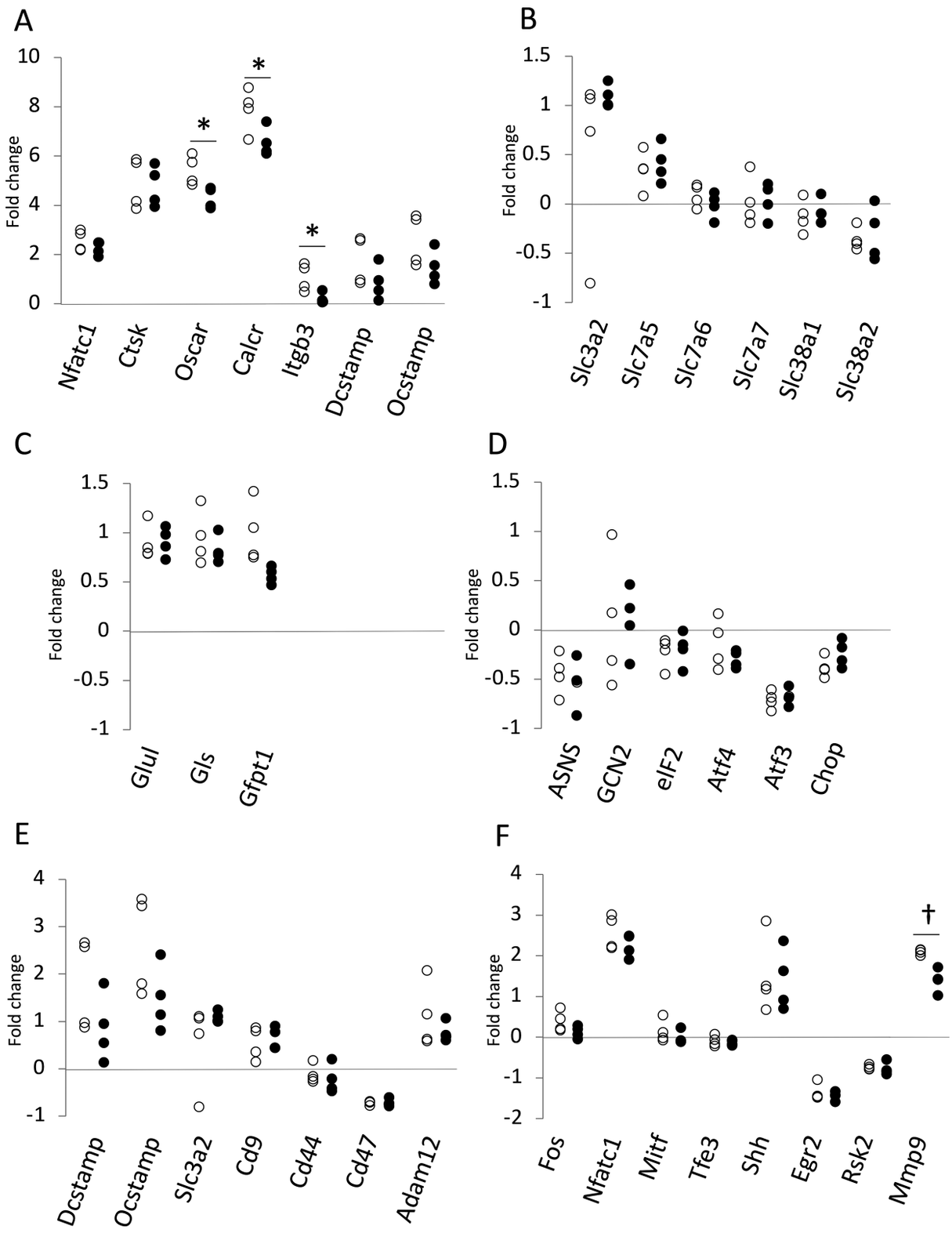

Figure 5. GeneChip analysis of *Slc1a5*$^{+/+}$ (W: open circles) and *Slc1a5*$^{-/-}$ (KO: closed circles) mice. Bone marrow–derived macrophages were prepared from bone marrow cells. After the bone marrow cells were cultured in the presence of mCSF for 3 d, and the bone marrow–derived macrophages among the adherent cells were collected. Osteoclasts were generated by culturing bone marrow–derived macrophages with mCSF and RANKL for 3 d. Gene expression was assayed on an Agilent gene expression system. The values are the ratio of change related to osteogenesis and glutamine metabolism genes in bone marrow–derived macrophages compared with osteoclasts. Each graph shows osteoclast related genes (A), glutamine transporter genes (B), glutamine metabolism genes (C), amino acid depletion genes (D), fusion factor genes (E), and target genes of ERK (F). *, $P < 0.05$; †, $P < 0.01$ between *Slc1a5*$^{+/+}$ mice and *Slc1a5*$^{-/-}$ mice ($n = 4$ per group).

was significantly lower in bone marrow cells isolated from *Slc1a5*$^{-/-}$ mice as compared with those isolated from *Slc1a5*$^{+/+}$ mice (Figure 5 F).

Immunoblotting analysis of signal events in bone marrow–derived macrophages. To investigate RANKL signaling, we determined the phosphorylation levels of signal transduction pathways related to osteoclast formation. Bone marrow cells were cultured for between 0 and 60 min after treatment with RANKL. The phosphorylation of ERK at 20 min (Figure 6 A), RelA at 5 min (Figure 6 C), and p70S6k at 20 and 60 min

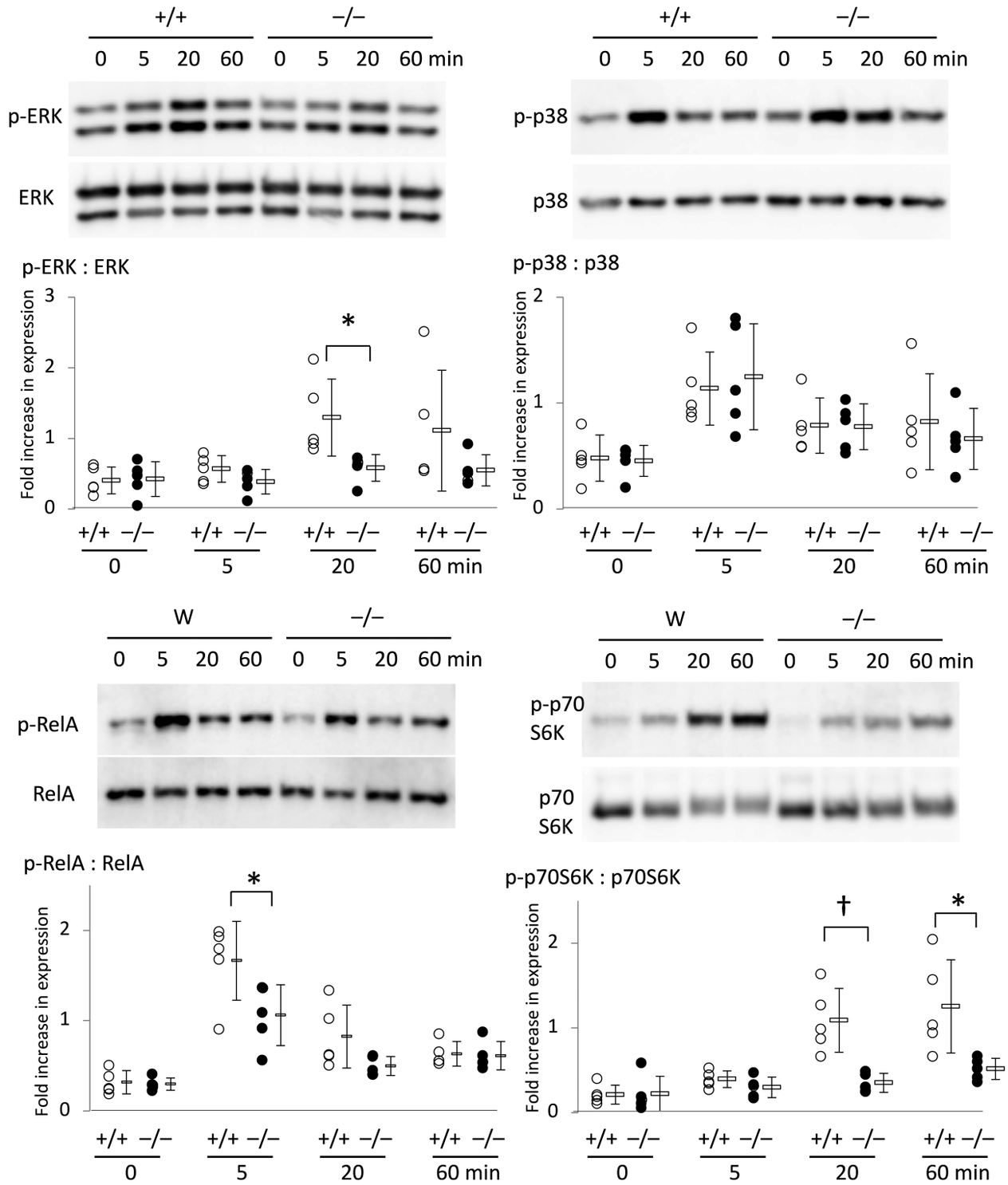

Figure 6. Immunoblotting analysis of signal events in *Slc1a5*$^{-/-}$ bone marrow–derived macrophages. Bone marrow–derived macrophages were cultured at various time points between 0 and 60 min after treatment with RANKL. Western blotting was performed by using the antibodies indicated, and protein levels were quantified by using NIH Image. *, $P < 0.05$; †, $P < 0.01$ between *Slc1a5* $^{+/+}$ mice and *Slc1a5*$^{-/-}$ mice (*n* = 5 per group).

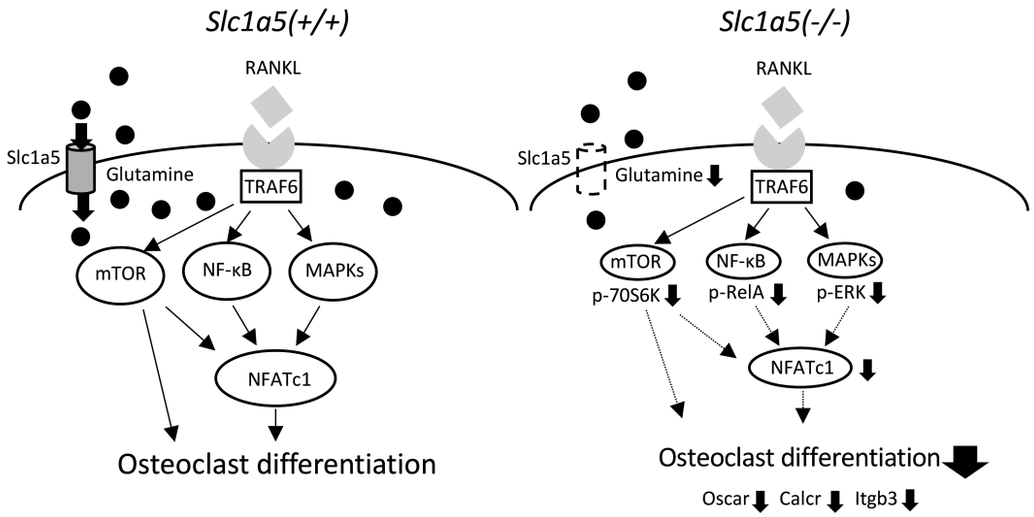

Figure 7. Signaling scheme of *Slc1a5*-mediated regulation in RANKL-induced osteoclast formation.

(Figure 6 D) was significantly lower in *Slc1a5*$^{-/-}$ bone marrow cells as compared with the *Slc1a5*$^{+/+}$ cells.

Discussion

To investigate the function of the sodium-dependent neutral amino acid transporter Slc1a5, we established *Slc1a5*-deficient (*Slc1a5*$^{-/-}$) mice. These mice did not show any obvious phenotypic abnormalities. This observation is consistent with that of a previously published study.[11,13] Our study found no significant difference in bone remodeling between *Slc1a5*$^{+/+}$ and *Slc1a5*$^{-/-}$ mice; therefore, further detailed studies are necessary to determine what extent Slc1a5 influences bone remodeling.

The current study demonstrated that *Slc1a5* deficiency impaired the osteoclast formation induced by exposure to RANKL. When bone marrow cells derived from *Slc1a5*$^{+/+}$ mice were stimulated by RANKL, many TRAP-positive osteoclasts were generated. However, osteoclastogenesis was significantly impaired in bone marrow cells derived from *Slc1a5*$^{-/-}$ mice. Actin ring formation and bone resorption activity occurred at very low levels in cells derived from *Slc1a5*$^{-/-}$ mice. The expression of genes involved in the signaling pathways induced by RANKL—ERK, NF-κB, mTOR, and NFATc1—was lower during osteoclastogenesis in *Slc1a5*$^{-/-}$ mice as compared with *Slc1a5*$^{+/+}$ mice. NFATc1 is a key transcription factor that mediates osteoclast differentiation and is regulated by phosphorylation involving distinct NFAT kinases. Our findings also show that *Slc1a5* also has an important role in osteoclastogenesis.

Slc1a5 belongs to the glutamate transporter family (*Slc1a*), and *Slc1a5* is the only glutamine transporter with a specific substrate-binding site.[17] Glutamine is important in a range of biologic functions, including energy supply, nucleotide biosynthesis, redox homeostasis, and apoptosis regulation. The rate of glutamine uptake in *Slc1a5*$^{-/-}$ bone marrow cells incubated with mCSF and RANKL was reduced to about 70% of that of *Slc1a5*$^{-/-}$ bone marrow cells in the presence of Na^+. This finding suggests that some glutamine was incorporated by other transporters such as *Slc38a1* and *Slc38a2*. This result is consistent with that of a previous report[11] focused on the B cells and fibroblasts of *Slc1a5*$^{-/-}$ mice.

A hypoxic environment contributes to the process of bone destruction by inducing osteoclast differentiation and hypoxia-stimulated glutamine consumption and glycolytic flux in osteoclasts. Glutamine uptake is therefore intimately related to the induction of osteoclastogenesis.[12] In previous studies,[3,4] *Slc1a5* deficiency was compensated for by increased levels of *Slc1a4*, *Slc38a1*, *Slc38a2*, and GCN2 in cancer cells. However, the expression of compensatory genes was not observed in RANKL-activated bone marrow cells derived from *Slc1a5*$^{-/-}$ mice in our study (Figure 5). These differences may be due to the characteristic differences between cancer cells and bone marrow cells.

Glutamine is essential for lymphocyte proliferation, cytokine production, and macrophage function. *Slc1a5* deficiency impaired the induction of Th1 and Th17 cells and inflammatory T cell responses in an experimental model of acquired immunity and autoimmunity.[13] *Slc1a5*-deficient T cells have defects in the activation of mTORC1 during T cell differentiation. However, in another study,[11] *Slc1a5* mutant mice with the same C57BL/6 background as our mice have normal B and T cell development and effector function. Genetic differences in mouse strains may affect the phenotype of *Slc1a5* deletion.

In the early stages of osteoclast differentiation, RANKL–RANK signaling is mediated by MAP kinases, NF-κB, and AP-1.[15] In mammalian cells, rapamycin-sensitive mTOR complex 1 is important for the phosphorylation and activation of p70S6k.[7] mTOR regulates osteoclast formation by modulating the C/EBPβ isoform ratio.[18] The subsequent signaling is characterized by amplifying NFATc1. In our results related to signal events, RANKL-induced phosphorylation of ERK, RelA, and p70S6K was suppressed during the trigger phase in *Slc1a5*-deficient bone marrow–derived macrophages. RelA, also known as p65, is a Rel-associated protein involved in NF-κB heterodimer formation, nuclear translocation, and activation. Our results indicate that *Slc1a5* mediates osteoclast differentiation in bone marrow cells by signaling through MAP, NFκB, and mTOR and that glutamine significantly affects signals related to osteoclasts (Figure 7).

In summary, our study demonstrates that *Slc1a5* is important in osteoclastogenesis in normal (noncancerous) cells. The role of glutamine transporters such as *Slc38a1* and *Slc38a2* should be analyzed further.

References

1. **Bothwell PJ, Kron CD, Wittke EF, Czerniak BN, Bode BP.** 2018. Targeted suppression and knockout of ASCT2 or LAT1 in epithelial and mesenchymal human liver cancer cells fail to inhibit growth. Int J Mol Sci **19:**1–25. https://doi.org/10.3390/ijms19072093.
2. **Boyle WJ, Simonet WS, Lacey DL.** 2003. Osteoclast differentiation and activation. Nature **423:**337–342. https://doi.org/10.1038/nature01658.
3. **Bröer A, Gauthier-Coles G, Rahimi F, van Geldermalsen M, Dorsch D, Wegener A, Holst J, Bröer S.** 2019. Ablation of the *ASCT2* (*SLC1A5*) gene encoding a neutral amino acid transporter reveals transporter plasticity and redundancy in cancer cells. J Biol Chem **294:**4012–4026. https://doi.org/10.1074/jbc.RA118.006378.
4. **Bröer A, Rahimi F, Bröer S.** 2016. Deletion of amino acid transporter ASCT2 (SLC1A5) reveals an essential role for transporters SNAT1 (SLC38A1) and SNAT2 (SLC38A2) to sustain glutaminolysis in cancer cells. J Biol Chem **291:**13194–13205. https://doi.org/10.1074/jbc.M115.700534.
5. **Cruzat V, Macedo Rogero M, Noel Keane K, Curi R, Newsholme P.** 2018. Glutamine: metabolism and immune function, supplementation and clinical translation. Nutrients **10:**1–31. https://doi.org/10.3390/nu10111564.
6. **Deitmer JW, Bröer A, Bröer S.** 2003. Glutamine efflux from astrocytes is mediated by multiple pathways. J Neurochem **87:**127–135. https://doi.org/10.1046/j.1471-4159.2003.01981.x.
7. **Glantschnig H, Fisher JE, Wesolowski G, Rodan GA, Reszka AA.** 2003. mCSF, TNFα and RANK ligand promote osteoclast survival by signaling through mTOR/S6 kinase. Cell Death Differ **10:**1165–1177. https://doi.org/10.1038/sj.cdd.4401285.
8. **Indo Y, Takeshita S, Ishii KA, Hoshii T, Aburatani H, Hirao A, Ikeda K.** 2013. Metabolic regulation of osteoclast differentiation and function. J Bone Miner Res **28:**2392–2399. https://doi.org/10.1002/jbmr.1976.
9. **Liu Y, Zhao T, Li Z, Wang L, Yuan S, Sun L.** 2018. The role of ASCT2 in cancer: A review. Eur J Pharmacol **837:**81–87. https://doi.org/10.1016/j.ejphar.2018.07.007.
10. **Lu H, Li X, Lu Y, Qiu S, Fan Z.** 2016. ASCT2 (SLC1A5) is an EGFR-associated protein that can be co-targeted by cetuximab to sensitize cancer cells to ROS-induced apoptosis. Cancer Lett **381:**23–30. https://doi.org/10.1016/j.canlet.2016.07.020.
11. **Masle-Farquhar E, Broer A, Yabas M, Enders A, Bröer S.** 2017. ASCT2 (SLC1A5)-deficient mice have normal b-cell development, proliferation, and antibody production. Front Immunol **8:**1–11. https://doi.org/10.3389/fimmu.2017.00549.
12. **Morten KJ, Badder L, Knowles HJ.** 2013. Differential regulation of HIF-mediated pathways increases mitochondrial metabolism and ATP production in hypoxic osteoclasts. J Pathol **229:**755–764. https://doi.org/10.1002/path.4159.
13. **Nakaya M, Xiao Y, Zhou X, Chang JH, Chang M, Cheng X, Blonska M, Lin X, Sun SC.** 2014. Inflammatory T cell responses rely on amino acid transporter ASCT2 facilitation of glutamine uptake and mTORC1 kinase activation. Immunity **40:**692–705. https://doi.org/10.1016/j.immuni.2014.04.007.
14. **Nicklin P, Bergman P, Zhang B, Triantafellow E, Wang H, Nyfeler B, Yang H, Hild M, Kung C, Wilson C, Myer VE, MacKeigan JP, Porter JA, Wang YK, Cantley LC, Finan PM, Murphy LO.** 2009. Bidirectional transport of amino acids regulates mTOR and autophagy. Cell **136:**521–534. https://doi.org/10.1016/j.cell.2008.11.044.
15. **Park JH, Lee NK, Lee SY.** 2017. Current understanding of RANK signaling in osteoclast differentiation and maturation. Mol Cells **40:**706–713. https:// doi.org/ 10.14348/molcells.2017.0225.
16. **Scalise M, Pochini L, Console L, Losso MA, Indiveri C.** 2018. The human SLC1A5 (ASCT2) amino acid transporter: from function to structure and role in cell biology. Front Cell Dev Biol **6:**1–17. https://doi.org/10.3389/fcell.2018.00096.
17. **Scopelliti AJ, Font J, Vandenberg RJ, Boudker O, Ryan RM.** 2018. Structural characterisation reveals insights into substrate recognition by the glutamine transporter ASCT2/SLC1A5. Nat Commun **9:**1–12. https://doi.org/10.1038/s41467-017-02444-w.
18. **Smink JJ, Begay V, Schoenmaker T, Sterneck E, de Vries TJ, Leutz A.** 2009. Transcription factor C/EBPβ isoform ratio regulates osteoclastogenesis through MafB. EMBO J **28:**1769–1781. https://doi.org/10.1038/emboj.2009.127.
19. **Takahashi N, Udagawa N, Tanaka S, Suda T.** 2003. Genetating murine osteoclasts from bone marrow. Methods Mol Med **80:**129–144.https:// doi.org/10.1385/1-59259-366-6:129.
20. **Tanimoto Y, Iijima S, Hasegawa Y, Suzuki Y, Daitoku Y, Mizuno S, Ishige T, Kudo T, Takahashi S, Kunita S, Sugiyama F, Yagami K.** 2008. Embryonic stem cells derived from C57BL/6J and C57BL/6N mice. Comp Med **58:**347–352.
21. **Tsumura H, Ito M, Li XK, Nakamura A, Ohnami N, Fujimoto J, Komada H, Ito Y**. 2012. The role of CD98hc in mouse macrophage functions. Cell Immunol **276:**128–134. https://doi.org/10.1016/j.cellimm.2012.04.012
22. **van Geldermalsen M, Wang Q, Nagarajah R, Marshall AD, Thoeng A, Gao D, Ritchie W, Feng Y, Bailey CG, Deng N, Harvey K, Beith JM, Selinger CI, O'Toole SA, Rasko JE, Holst J.** 2015. ASCT2/SLC1A5 controls glutamine uptake and tumour growth in triple-negative basal-like breast cancer. Oncogene **35:**3201–3208. https://doi.org/10.1038/onc.2015.381.
23. **Wang Q, Hardie RA, Hoy AJ, van Geldermalsen M, Gao D, Fazli L, Sadowski MC, Balaban S, Schreuder M, Nagarajah R, Wong JJ, Metierre C, Pinello N, Otte NJ, Lehman ML, Gleave M, Nelson CC, Bailey CG, Ritchie W, Rasko JE, Holst J.** 2015. Targeting ASCT2-mediated glutamine uptake blocks prostate cancer growth and tumour development. J Pathol **236:**278–289. https://doi.org/10.1002/path.4518.
24. **Yu Y, Newman H, Shen L, Sharma D, Hu G, Mirando AJ, Zhang H, Knudsen E, Zhang GF, Hilton MJ, Karner CM.** 2019. Glutamine metabolism regulates proliferation and lineage allocation in skeletal stem cells. Cell Metab **29:**966–978.e4. https://doi.org/10.1016/j.cmet.2019.01.016.